Synthesis, Characterization, and Theoretical Study of Stable Isomers of C70(CF3)n (n = 2, 4, 6, 8, 10)

ARTICLE *in* CHEMISTRY - A EUROPEAN JOURNAL · MAY 2006

Impact Factor: 5.73 · DOI: 10.1002/chem.200501346 · Source: PubMed

13 AUTHORS, INCLUDING:

Alexey A Goryunkov
Lomonosov Moscow State University
72 PUBLICATIONS **859** CITATIONS
SEE PROFILE

Ilya N Ioffe
Lomonosov Moscow State University
64 PUBLICATIONS **1,224** CITATIONS
SEE PROFILE

Alexey A Popov
Leibniz Institute for Solid State and Materia…
188 PUBLICATIONS **3,412** CITATIONS
SEE PROFILE

Igor V Kuvychko
Colorado State University
62 PUBLICATIONS **1,120** CITATIONS
SEE PROFILE

CHEMISTRY
A EUROPEAN JOURNAL

DOI: 10.1002/chem.200501346

Synthesis, Characterization, and Theoretical Study of Stable Isomers of $C_{70}(CF_3)_n$ ($n = 2, 4, 6, 8, 10$)

Eugenii I. Dorozhkin,[b] Daria V. Ignat'eva,[b] Nadezhda B. Tamm,[b] Alexey A. Goryunkov,[b] Pavel A. Khavrel,[b] Ilya N. Ioffe,[b] Alexey A. Popov,[b] Igor V. Kuvychko,[a] Alexey V. Streletskiy,[b] Vitaliy Y. Markov,[b] Johann Spandl,[c] Steven H. Strauss,*[a] and Olga V. Boltalina*[a, b]

Abstract: Reaction of C_{70} with ten equivalents of silver(I) trifluoroacetate at 320–340 °C followed by fractional sublimation at 420–540 °C and HPLC processing led to the isolation of a single abundant isomer of $C_{70}(CF_3)_n$ for $n = 2$, 4, 6, and 10, and two abundant isomers of $C_{70}(CF_3)_8$. These six compounds were characterized by using matrix-assisted laser desorption ionization (MALDI) mass spectrometry, 2D-COSY and/or 1D ^{19}F NMR spectroscopy, and quantum-chemical calculations at the density functional theory (DFT) level. Some were also characterized by Raman spectroscopy. The addition patterns for the isolated compounds were unambiguously found to be C_1-7,24-$C_{70}(CF_3)_2$, C_1-7,24,44,47-$C_{70}(CF_3)_4$, C_2-1,4,11,19,31,41-$C_{70}(CF_3)_6$, C_s-1,4,11,19,31,41,51,64-$C_{70}(CF_3)_8$, C_2-1,4,11,19,31,41,51,60-$C_{70}(CF_3)_8$, and C_1-1,4,10,19,25,41,49,60,66,69-$C_{70}(CF_3)_{10}$ (IUPAC numbering). Except for the last compound, which is identical to the recently reported, crystallographically characterized $C_{70}(CF_3)_{10}$ derivative prepared by a different synthetic route, these compounds have not previously been shown to have the indicated addition patterns. The largest relative yield under an optimized set of reaction conditions was for the C_s isomer of $C_{70}(CF_3)_8$ (ca. 30 mol% of the sublimed mixture of products based on HPLC integration). The results demonstrate that thermally stable $C_{70}(CF_3)_n$ isomers tend to have their CF_3 groups arranged on isolated *para*-$C_6(CF_3)_2$ hexagons and/or on a ribbon of edge-sharing *meta*- and/or *para*-$C_6(CF_3)_2$ hexagons. For C_s- and C_2-$C_{70}(CF_3)_8$ and for C_2-$C_{70}(CF_3)_6$, the ribbons straddle the C_{70} equatorial belt; for C_1-$C_{70}(CF_3)_4$, the *para–meta–para* ribbon includes three polar hexagons; for C_1-7,24-$C_{70}(CF_3)_2$, the *para*-$C_6(CF_3)_2$ hexagon includes one of the carbon atoms on a C_{70} polar pentagon. The 10.3–16.2 Hz $^7J_{F,F}$ NMR coupling constants for the end-of-ribbon CF_3 groups, which are always *para* to their nearest-neighbor CF_3 group, are consistent with through-space Fermi-contact interactions between the fluorine atoms of proximate, rapidly rotating CF_3 groups.

Keywords: density functional calculations · fullerenes · isomers · through-space interactions · trifluoromethyl

[a] I. V. Kuvychko, Prof. S. H. Strauss, Prof. O. V. Boltalina
Department of Chemistry
Colorado State University
Fort Collins, CO 80523 (USA)
Fax: (+1) 970-491-1801
E-mail: steven.strauss@colostate.edu
ovbolt@lamar.colostate.edu

[b] E. I. Dorozhkin, D. V. Ignat'eva, Dr. N. B. Tamm, Dr. A. A. Goryunkov, P. A. Khavrel, Dr. I. N. Ioffe, Dr. A. A. Popov, Dr. A. V. Streletskiy, Dr. V. Y. Markov, Prof. O. V. Boltalina
Chemistry Department
Moscow State University
Moscow 119992 (Russia)

[c] Dr. J. Spandl
Institut für Chemie und Biochemie
der Freie Universität
Berlin 14195 (Germany)

Introduction

In 2001 we reported[1] that poly(trifluoromethyl)fullerenes can be synthesized by reacting C_{60} or C_{70} with various transition-metal trifluoroacetate (TFA) salts at elevated temperatures (this discovery was subsequently patented[2]). The products consisted of a wide range of $C_{60,70}(CF_3)_n$ derivatives with $n \leq 22$.[1] We recently published a 380/500 °C fractional sublimation procedure for a particular $C_{60}(CF_3)_n$ mixture of products (C_{60}, AgTFA, 280 °C) that resulted in fewer,[3] more stable[4] isomers of $C_{60}(CF_3)_{2,4,6,8,10}$ as the predominant isolated products. This greatly simplified the HPLC purification and spectroscopic characterization of individual isomers of $C_{60}(CF_3)_{2,4,6}$.[3] Without fractional sublimation, the tol-

uene-extractable mixture of products included many more $C_{60}(CF_3)_n$ derivatives ($n \leq 14$) as well as a large number of $C_{60}(CF_3)_nH_m$ derivatives, many of which could only be isolated as mixtures of products even after HPLC processing.[5,6] Application of our original AgTFA synthetic methodology[1,2] without high-temperature fractional sublimation to the polytrifluoromethylation of C_{70} also resulted in complex mixtures of $C_{70}(CF_3)_n$ and $C_{70}(CF_3)_nH_m$ derivatives.[5,7]

We now report that high-temperature fractional sublimation followed by HPLC processing of C_{70}/AgTFA reaction mixtures (with reaction temperatures of 320–340 °C) leads to the isolation of milligram amounts of a single abundant isomer of $C_{70}(CF_3)_2$, $C_{70}(CF_3)_4$, $C_{70}(CF_3)_6$, $C_{70}(CF_3)_8$, and $C_{70}(CF_3)_{10}$, and a smaller amount of a second isomer of $C_{70}(CF_3)_8$. A combination of ^{19}F NMR and Raman spectroscopy and quantum-chemical calculations at the density functional theory (DFT) level demonstrate that the isolated compounds are among the most stable isomers, if not the most stable isomer, for each $C_{70}(CF_3)_n$ composition investigated.

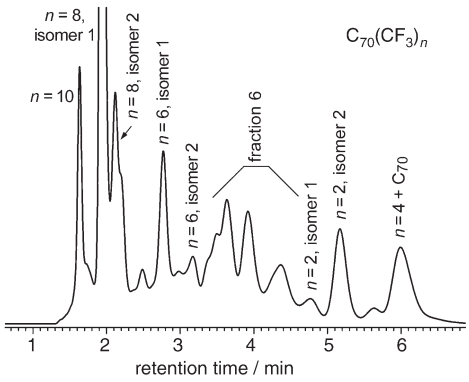

Figure 1. HPLC chromatogram of the sublimed (480 °C) products (10 mg) from the reaction of C_{70} (100 mg) and AgTFA (267 mg) at 320 °C for 1 h. The integrated intensity of the peak for the second fraction, which contained $\geq 90\%$ C_s-$C_{70}(CF_3)_8$, was 31 % of the total integrated intensity.

Experimental Section

Reagents and solvents: HPLC-grade toluene and heptane (Fisher), hexafluorobenzene (Aldrich), [D_6]benzene (Cambridge Isotopes), silver(I) trifluoroacetate (AgTFA, Sigma Aldrich, ACS Reagent Grade), *trans*-2-[3-(4-*tert*-butylphenyl)-2-methyl-2-propenylidene]malononitrile (DCTB, Fluka), and KBr (Sigma Aldrich, $\geq 99\%$, FTIR grade) were used as received. The fullerene C_{70} (98 %) was a gift from Term-USA.

Spectroscopic characterization: Samples for negative-ion matrix-assisted laser desorption ionization (MALDI) mass spectrometry were prepared as follows. An HPLC-purified sample of a particular $C_{70}(CF_3)_n$ derivative (1 equiv) and the matrix material *trans*-2-[3-(4-*tert*-butylphenyl)-2-methyl-2-propenylidene]malononitrile (DCTB; 1000 equiv) were dissolved in toluene and deposited on the target. The MALDI mass spectra were recorded in the reflectron mode using one of the time-of-flight mass spectrometers (Kratos Analytical Vision MALDI; Bruker AutoFlex MALDI). A 337 nm dinitrogen laser was used for target activation. Each mass spectrum was the average of more than 100 laser shots. Samples for ^{19}F NMR spectroscopy were solutions in [D_6]benzene containing a small amount of hexafluorobenzene as an internal standard ($\delta = -164.9$ ppm). One- and two-dimensional gCOSY spectra were recorded by using a Varian INOVA-unity 400 spectrometer operating at 367.45 MHz. Raman spectra of purified samples of the most abundant isomers of $C_{70}(CF_3)_4$ and $C_{70}(CF_3)_8$ were recorded by using a Bruker RFS 100 FT-Raman spectrometer operating at 3 cm^{-1} resolution.

Preparation and purification of $C_{70}(CF_3)_n$ (n = 2, 4, 6, 8, 10): In a typical synthesis, a mixture of C_{70} (112 mg, 0.133 mmol) and AgTFA (299 mg, 1.35 mmol) was thoroughly ground together and transferred to a Pyrex tube that was subsequently sealed in a copper tube (the AgTFA/C_{70} mole ratio in this case was 10:1; other mole ratios investigated were 5:1, 30:1, and 60:1). The sealed reaction mixture was heated to 320–340 °C for 1–2 h in a tube furnace. The product mixture was sublimed under vacuum (10^{-2} torr) at 420, 480, and 520 °C (in one synthesis the product mixture was sublimed a fourth time at 540 °C). The sublimate after each of the first two (or three) stages of this process was isolated separately before proceeding to the next higher temperature.

Portions of the sublimates (ca. 10 mg) were dissolved in toluene (ca. 2 mL) and were analyzed and purified using a Waters Breeze HPLC system (4.6 mm i.d. × 25 cm Cosmosil Buckyprep column (Nacalai Tesque); toluene eluent, flow rate = 2 mL min^{-1}; $\lambda = 290$ nm detection). A typical HPLC trace is shown in Figure 1. In this particular example, the nine indicated fractions were collected and subsequently analyzed by using MALDI mass spectrometry. In some cases a second stage of HPLC purification was employed. Milligram samples of the most abundant isomers of $C_{70}(CF_3)_n$ (n = 2, 4, 6, 8, and 10) plus a second, relatively abundant, isomer of $C_{70}(CF_3)_8$ were isolated from the HPLC fractions and were characterized by using 1D and 2D gCOSY ^{19}F NMR spectroscopy. Some samples were also characterized by using Raman spectroscopy.

A series of standard concentrations of C_{70} and abundant isomer 1 of $C_{70}(CF_3)_8$ (C_s-$C_{70}(CF_3)_8$) were used to determine the ratio of extinction coefficients (ε) for these two compounds in toluene at $\lambda = 290$ nm ($\varepsilon(C_{70})/\varepsilon(C_{70}(CF_3)_8) = 1.47$). By assuming an additivity relationship between pairs of CF_3 groups and relative changes in extinction coefficient, we estimated the relative amount of C_s-$C_{70}(CF_3)_8$ in each of the sublimation fractions.

Quantum-chemical calculations: Molecular structures and harmonic vibrational frequencies were calculated at the DFT level of theory with the PRIRODA package[8] by using the GGA functional of Perdew, Burke, and Ernzerhof (PBE).[9] The TZ2P-quality Gaussian basis set {6,1,1,1,1,1/4,1,1/1,1} was used for carbon and fluorine atoms. The quantum-chemical code employed expansion of the electron density in an auxiliary basis set to accelerate the evaluation of the Coulomb and exchange-correlation terms. Raman intensities were computed numerically at the PBE/6-31G level by employing the GAMESS(US) quantum-chemical package.[10,11] AM1 calculations were also performed with GAMESS(US).

Results and Discussion

A more selective synthesis of $C_{70}(CF_3)_n$ derivatives: In exploring the chemical reactivities of new compounds such as fullerenes, a chemist might go through different stages pursuing different goals. Initially, different synthetic methodologies might be investigated in order to see which reactions and sets of conditions are viable ways to prepare new classes of derivatives, but without any particular compound as the target. This exploratory stage might be followed by the development of purification procedures and analytical methods so that whatever new compounds are produced can be identified, purified, and fully characterized. Finally, the ultimate goal of the synthetic chemist is to use this information to prepare a specific target compound in practical amounts and with high purity.

Several reaction methodologies have been explored for the preparation and isolation of poly(perfluoroalkyl)fullerenes. The pioneering work of the DuPont group showed that thermal and photochemical reactions of R_fI reagents (R_f = a perfluoroalkyl group) and C_{60} produced complex mixtures of compounds such as $C_{60}(R_f)_n$ and $C_{60}(R_f)_nH_m$ (the source of hydrogen atoms was the organic solvents used, either benzene or 1,2,4-trichlorobenzene).[12] Shinohara and co-workers later used a similar photochemical reaction followed by multistage HPLC purification to isolate approximately 1 mg of $La@C_{82}(C_8F_{17})_2$.[13] We have recently explored thermal reactions of volatile R_fI reagents and solid empty fullerenes and have isolated and structurally characterized two new compounds with unprecedented structures, 1,3,7,10,14,17,23,28,31,40-$C_{60}(CF_3)_{10}$[14] and 1,4,10,19,25,41,49,60,66,69-$C_{70}(CF_3)_{10}$.[15] In addition, we have reported the use of silver(I) trifluoroacetate (AgTFA) to convert $Y@C_{82}$ into two isomers of $Y@C_{82}(CF_3)_5$, the first diamagnetic exohedral derivatives of $Y@C_{82}$.[16] The last example used the general synthetic methodology that is the subject of this paper, that is, the solid-state reaction of fullerenes with a metal trifluoroacetate salt at temperatures known to cause the thermal decomposition of the metal trifluoroacetate and the concomitant formation of trifluoromethyl radicals.[1,2]

The solid-state reaction of C_{60} and C_{70} with silver(I) trifluoroacetate (AgTFA) at 300–320 °C is known to produce a wide variety of fullerene$(CF_3)_n$ compositions and isomers.[1–3,5–7] In one study, 45 individual $C_{70}(CF_3)_n$ derivatives were identified, although only a few could be isolated with $\geq$85% purity.[7] As an example from our work, the bottom HPLC trace in Figure 2 shows the high degree of molecular complexity present in the products when a mixture of C_{70} and AgTFA was heated for 1 h at 320 °C. Our goal is not to discover how many different fullerene$(CF_3)_n$ compounds can be formed in one reaction (this had already been determined in the DuPont work[12]), but to find conditions for the isolation of a small number of abundant products in amounts large enough so that their chemical properties, not only their spectroscopic properties, can be investigated. An ancillary goal is to discover which fullerene$(CF_3)_n$ isomer represents the thermodynamically most stable isomer observed for a given fullerene and a given value of n, as opposed to other observed isomers that have higher ΔH_f° (or ΔG_f°) values but are kinetically stable at the reaction temperature. This is an important issue in fullerene science and technology because all possible isomers of fullerene$(X)_n$ compositions cannot be investigated by quantum chemical calculations, even when $n = 4$ (e.g., there are nearly 46000 possible isomers of $C_{70}H_4$ and nearly 5×10^8 isomers of $C_{70}H_8$[17]). Fullerene theorists must rely on the isolation and unambiguous characterization of new derivatives by synthetic chemists to point out which of the multitude of isomers are worth calculating.

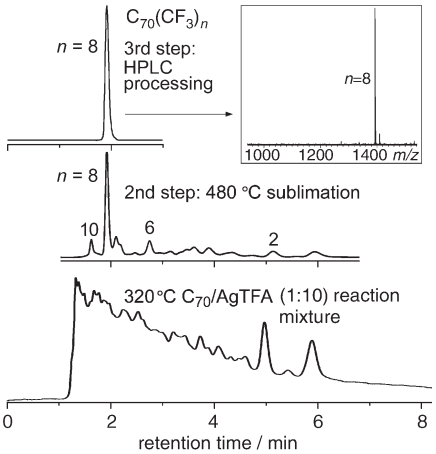

Figure 2. HPLC chromatograms of the toluene-extractable crude product mixture from the reaction of C_{70} (100 mg) and AgTFA (267 mg) at 320 °C for 1 h (bottom), after fractional sublimation (middle), and after HPLC purification (top). The inset shows the mass spectrum of HPLC-purified C_s-$C_{70}(CF_3)_8$.

Our previous work with the C_{60}/AgTFA system showed that high-temperature sublimation of the product mixture led to the isolation of fewer, presumably more stable, products than are present in the product mixture before high-temperature processing.[3] We now report that high-temperature sublimation leads to significantly fewer products in the C_{70}/AgTFA system. This can be clearly seen by comparing the bottom and middle HPLC traces in Figure 2. The 480 °C sublimation fraction in this example contains an abundant isomer of $C_{70}(CF_3)_8$ that was isolated with $\geq$90% purity after only one cycle of HPLC purification, as shown in the top HPLC trace and the MALDI-MS inset in Figure 2. The peak intensity of this isomer in the middle HPLC trace is 31% of the total integrated intensity.

The negative-ion MALDI mass spectrum in Figure 2 demonstrates that little or no fragmentation of $C_{70}(CF_3)_8$ occurred upon ionization when *trans*-2-[3-(4-*tert*-butylphenyl)-2-methyl-2-propenylidene]malononitrile (DCTB) was used as the MALDI matrix. This was also true of the other C_{70}-$(CF_3)_n$ compounds analyzed in this work. In contrast, 70 eV electron-ionization mass spectrometry causes significant fragmentation of $C_{60,70}(CF_3)_n$ derivatives upon ionization.[1,7] The matrix material DCTB has also been used to obtain MALDI mass spectra of $C_{60}F_n$ derivatives (n = 18, 36, 48) and $C_{60}Cl_6$ with relatively small degrees of fragmentation.[18]

Silver(I) trifluoroacetate is known to decompose to form trifluoromethyl radicals at 300 °C [Eq. (1)].[19] The formation of $C_{70}(CF_3)_n$ derivatives may very well take place by the sequential addition of $CF_3^\bullet$ radicals [Eq. (2)], although this is by no means proven:

$$Ag(CF_3CO_2) \xrightarrow{300\,^oC} Ag(s) + CO_2(g) + CF_3^\bullet(g) \quad (1)$$

$$nCF_3^\bullet(g) + C_{70}(s) \xrightarrow{300\,^oC} C_{70}(CF_3)_n \quad (2)$$

Different AgTFA/C_{70} mole ratios were investigated. Figure 3 shows HPLC traces and MALDI mass spectra of the toluene-extractable crude reaction mixtures from 60:1, 10:1, and 5:1 mole ratio AgTFA/C_{70} reactions (320 °C for

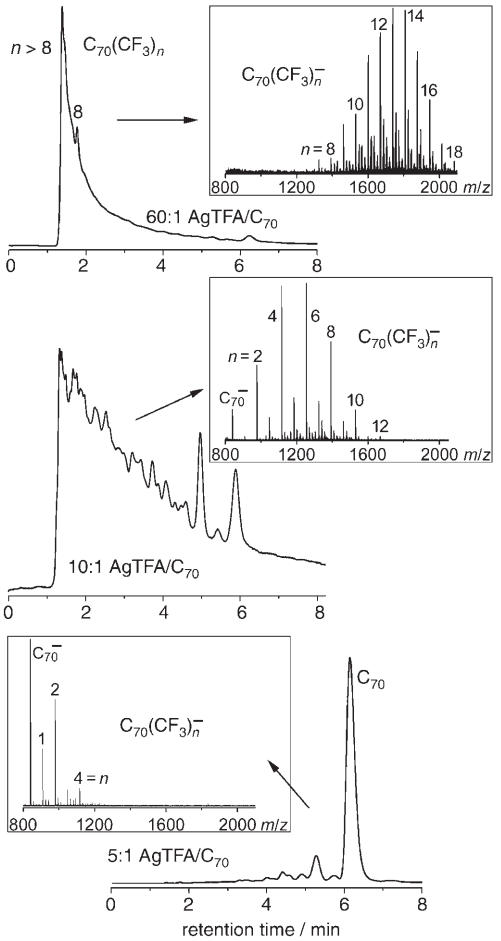

Figure 3. HPLC chromatograms and MALDI mass spectra of the toluene-extractable crude product mixtures from 60:1 (top), 10:1 (middle), and 5:1 (bottom) AgTFA/C_{70} mole-ratio reactions (320 °C for 1 h). The 30:1 mole-ratio product mixture gave a chromatogram similar to the 60:1 product mixture.

1 h). As expected, the higher the AgTFA/C_{70} mole ratio, the more CF_3 groups were added to C_{70} on average. The predominant $C_{70}(CF_3)_n$ products were $C_{70}(CF_3)_{12}$ and $C_{70}(CF_3)_{14}$ when the AgTFA/C_{70} mole ratio was 60:1, and there was, at most, a small amount of unreacted C_{70}. On the other hand, the predominant $C_{70}(CF_3)_n$ product was $C_{70}(CF_3)_2$ when the mole ratio was 5:1, and there was a significant amount of unreacted C_{70} in the toluene-extractable crude reaction mixture. Also present in all three reaction mixtures were significant quantities of $C_{70}(CF_3)_nH_m$, $C_{70}(CF_3)_nO_x$, and $C_{70}(CF_3)_nH_mO_x$ derivatives for both even and odd values of n. The source of the hydrogen and oxygen atoms might be adventitious water and/or dioxygen. Significant amounts of poly(trifluoromethyl)fullerene hydrides were also observed by other investigators of AgTFA/fullerene reactions.[6]

The 10:1 AgTFA/C_{70} mole ratio appeared to be the most promising as far as generating the set of compounds $C_{70}(CF_3)_n$ with $2 \le n \le 10$, the set of compositions we were most interested in studying. We applied the high-temperature sublimation procedure to several reaction mixtures, using a number of temperatures between 420 and 540 °C. The results for three reaction/sublimation sequences are listed in Table 1. HPLC traces and MALDI mass spectra for reaction/sublimation sequence 2 are shown in Figure 4. The 420 °C sublimate contained more $C_{70}(CF_3)_8$ and $C_{70}(CF_3)_{10}$ relative to $C_{70}(CF_3)_2$ and $C_{70}(CF_3)_4$ than did the 480 °C sublimate because, as previously found, fullerene$(CF_3)_n$ derivatives become more volatile as n increases, at least up to n =

Table 1. Relative yields of C_s-$C_{70}(CF_3)_8$ in three reaction/sublimation procedures.

Reaction		T_{subl}[a] [°C]	t_{subl}[b] [h]	m_{total}[c] [mg]	C_s-$C_{70}(CF_3)_8$ rel amount [%]	% yield
1	112 mg C_{70},	420	2	5	26	
	299 mg AgTFA,	460	2	34	33	32
	340 °C, 3 h	520	2	30	33	
2	100 mg C_{70},	420	1	5	33	
	267 mg AgTFA,	480	1	29	31	
	320 °C, 1 h	520	1	7	18	28
		540	1	1	2	
3	145 mg C_{70},	420	1	22	28	
	392 mg AgTFA,	480	1	30	27	26
	320 °C, 1 h	520	1	8	19	

[a] Sublimation temperature. [b] Sublimation time. [c] Total sublimate mass collected.

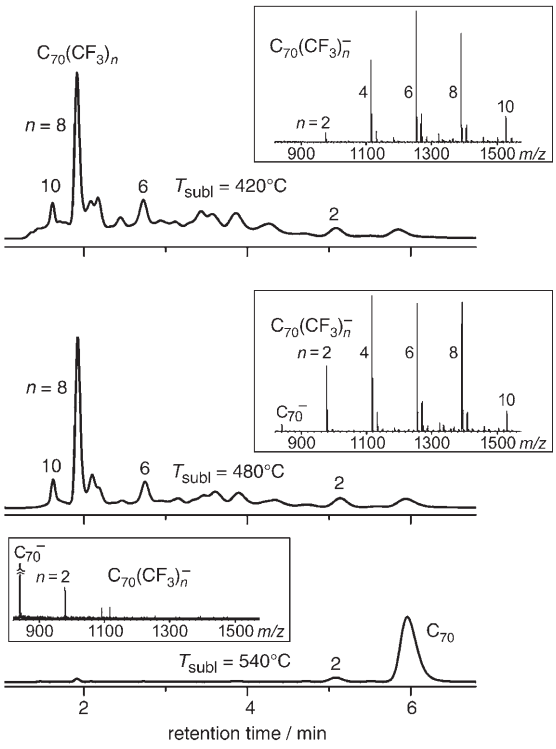

Figure 4. HPLC chromatograms and MALDI mass spectra of the 420 (top), 480 (middle), and 540 °C (bottom) sublimation fractions of the products from reaction sequence 2 (see Table 1).

10.[3,14] The 540 °C sublimate contained essentially $C_{70}(CF_3)_2$ and unreacted C_{70}.

In addition to separating the various $C_{70}(CF_3)_n$ derivatives from nonvolatile reaction products, from unreacted C_{70}, and to some extent from each other, the high-temperature sublimations significantly reduced the amounts of the undesired byproducts $C_{70}(CF_3)_nH_m$, $C_{70}(CF_3)_nO_x$, and $C_{70}(CF_3)_nH_mO_x$. This could be because many of these derivatives are nonvolatile or, more likely, because they are thermally labile and decompose at temperatures above 400 °C. In addition, it is possible that there are more isomers for a given value of *n* before sublimation than after sublimation (i.e., that less stable $C_{70}(CF_3)_n$ isomers rearrange to more stable isomers above 400 °C), but we are not yet in a position to rigorously test this hypothesis.

An expanded view of the 480 °C sublimate HPLC trace from reaction/sublimation sequence 2 is presented in Figure 1. The identities of the compounds in each fraction are listed in Table 2. Fraction 6 was collected as a group of poorly resolved peaks and subjected to chromatography a second time (not shown).

Table 2. Composition of the HPLC fractions shown in Figure 1.[a]

Fraction	t_R[b] [min]	$C_{70}(CF_3)_n$ compound present[c]
1	1.6	C_1-$C_{70}(CF_3)_{10}$
2	1.9	C_s-$C_{70}(CF_3)_8$
3	2.1	C_2-$C_{70}(CF_3)_8$
4	2.7	C_2-$C_{70}(CF_3)_6$
5	3.1	$C_{70}(CF_3)_6$ (unknown isomer)
6-1	3.3	$C_{70}(CF_3)_6O$ (unknown isomer)
6-2	3.6	$C_{70}(CF_3)_4O$ (unknown isomer)
6-3, 6-4	3.8–4.4	$C_{70}(CF_3)_{4,6}$, $C_{70}(CF_3)_{4,6}O$ (unknown isomers)
7	4.7	$C_{70}(CF_3)_2$ (unknown isomer)
8	5.1	C_1-$C_{70}(CF_3)_2$
9	5.8–6.0	C_1-$C_{70}(CF_3)_4$, C_{70}

[a] 4.6 mm i.d. × 25 cm Cosmosil Buckyprep column; toluene eluent, flow rate 2 mL min^{-1}. [b] Retention time. [c] Composition determined by MALDI-MS; symmetry and addition pattern determined by ^{19}F NMR spectroscopy.

AM1 and DFT study of $C_{70}(CF_3)_n$ and selected $C_{70}X_n$ derivatives (X = H, F, Br, Ph) and ^{19}F NMR spectra of $C_{70}(CF_3)_n$ (n = 2, 4, 6, 8, 10)

Theoretical results: In 1999 Clare and Kepert published their seminal AM1 quantum-chemical study of $C_{70}X_n$ derivatives in which the most stable isomers of all that were considered for a given composition were predicted (X = H, F, Br, Ph; n = 2, 4, 6, 8, 10, 12).[20] At that time, experimental data on $C_{70}X_n$ derivatives were limited to two isomers of $C_{70}H_2$,[21,22] six isomers of $C_{70}H_4$,[22] and one isomer each of $C_{70}Cl_{10}$,[23,24] $C_{70}Ph_8$,[25] and $C_{70}Ph_{10}$.[25] (We are only considering derivatives in which X is a monatomic or polyatomic substituent that forms a 2c–2e σ bond to a single cage-carbon atom.) In any theoretical study of fullerene(X)$_n$ derivatives with $n \geq 4$, time constraints limit the number of isomers that can be investigated to a small fraction of all possible isomers. Therefore, all theoretical studies must impose a set of limiting rules, the first two of which are usually that the derivatives 1) must have the same underlying cage structure as the fullerene starting material and 2) must have closed-shell electron configurations. A further limitation imposed by Clare and Kepert was to investigate only the most stable $C_{70}H_n$ addition patterns determined in their study for derivatives with X = F, Br, and Ph.[20] Other limiting rules were used in a MNDO study, in which the only isomers of $C_{70}Cl_{10}$ considered 1) were consistent with the observed ^{13}C NMR spectrum (C_s symmetry with five symmetry-related pairs of sp^3 carbon atoms), 2) had no double bonds in pentagons, and 3) had at most two adjacent sp^3 carbon atoms.[24]

To test our hypothesis that the 420–520 °C temperature range used for the fractional sublimation of $C_{70}(CF_3)_n$ derivatives in this study caused rearrangement of less stable isomers of a given composition to fewer, more stable isomers (the most abundant of which we have isolated and characterized by using ^{19}F NMR spectroscopy), we carried out quantum-chemical calculations on a relatively large number of possible isomers at the AM1 level and on a smaller number of possible isomers at the DFT level. All 143 isomers of $C_{70}(CF_3)_2$ were considered at the AM1 level, as were more than 1700 isomers of $C_{70}(CF_3)_4$, more than 900 isomers of $C_{70}(CF_3)_6$, and more than 6000 isomers of C_{70}-$(CF_3)_8$. The DFT calculations were normally restricted to isomers that had AM1 ΔH_f° values no more than 100 kJ mol^{-1} above the most stable AM1 isomer. In addition to excluding isomers that do not possess the D_{5h}-IPR C_{70} core (IPR = isolated pentagon rule) and that have open-shell electron configurations, we also excluded isomers 1) with one or more CF_3 groups on triple-hexagon junctions, 2) with isolated *meta*-$C_6(CF_3)_2$ hexagons, 3) with ribbons of edge-sharing *meta*- and/or *para*-$C_6(CF_3)_2$ hexagons that terminate with a *meta*-$C_6(CF_3)_2$ hexagon, and 4) with ribbons that have consecutive *meta*-$C_6(CF_3)_2$ hexagons. These limitations were deemed appropriate because $C_{60}(CF_3)_{2,4,6}$ isomers with the excluded addition patterns were previously shown by DFT calculations to be much less stable than isomers with 1) isolated *para*-$C_6(CF_3)_2$ hexagons, 2) ribbons that terminate with *para*-$C_6(CF_3)_2$ hexagons, or 3) ribbons not containing *-mm-* sequences.[4] The results of selected DFT calculations are shown in Figure 5, which also shows the Schlegel diagram and nomenclature abbreviation for each addition pattern. For comparison, we also carried out AM1 and DFT calculations on several isomers of $C_{70}H_n$, $C_{70}F_n$, $C_{70}Cl_n$, $C_{70}Br_n$, and $C_{70}Ph_n$ that had not been previously considered theoretically. These results are compared with those for C_{70}-$(CF_3)_n$ isomers with the same addition pattern in Table 3, which also lists the number of (usually destabilizing) double bonds in pentagons (dbip) for each isomer.

NMR spectra: Based on 1D and 2D ^{19}F NMR spectroscopic data and DFT calculations, we previously proposed that most fullerene$(CF_3)_n$ compounds prepared or purified at temperatures ≥380 °C have their CF_3 groups arranged on a

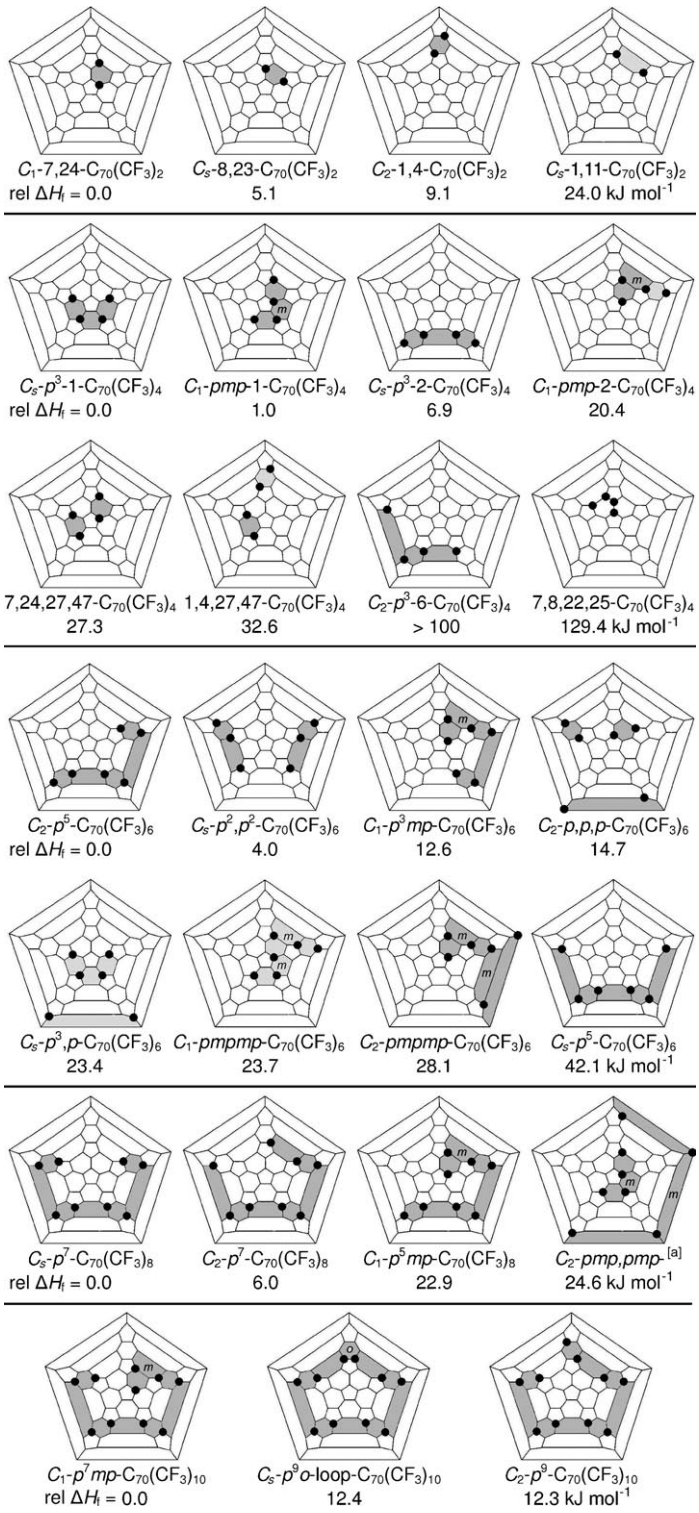

Figure 5. Schlegel diagrams and DFT-predicted relative ΔH_f° values (in kJ mol^{-1}) for selected isomers of $C_{70}(CF_3)_n$ (n = 2, 4, 6, 8, 10). [a] The structure labeled "C_2-*pmp,pmp*-" is C_2-*pmp,pmp*-$C_{70}(CF_3)_8$. IUPAC lowest-locant abbreviations: C_s-p^3-1 = 8,23,27,44; C_1-*pmp*-1 = 7,24,44,47; C_s-p^3-2 = 1,4,11,31; C_1-*pmp*-2 = 1,4,10,25; C_s-p^3-6 = 1,4,11,19; C_2-p^5 = 1,4,11,19,31,41; C_s-p^2,p^2 = 1,4,11,58,61,64; C_s-p^3,*p* = 8,16,23,27,33,47; C_1-p^3mp = 1,4,10,19,25,41; C_2-*p,p,p* = 1,4,24,34,43,52; C_1-*pmpmp* = 1,4,10,23,25,44; C_2-*pmpmp* = 1,4,10,18,25,35; C_s-p^5 = 1,4,11,19,31,51; C_s-p^7 = 1,4,11,19,31,41,51,64; C_2-p^7 = 1,4,11,19,31,41,51,60; C_1-p^5mp = 1,4,10,19,25,41,60,69; C_s-*pmp,pmp* = 7,17,24,36,44,47,53,56; C_1-p^7mp = 1,4,10,19,25,41,49,60,66,69; C_s-p^9o-loop = 1,4,11,19,29,41,49,60,66,69; C_2-p^9 = 1,4,11,19,31,41,49,60,66,69.

continuous ribbon of edge-sharing *meta*- and/or *para*-$C_6(CF_3)_2$ hexagons (fullerene = C_{60}, C_{70}, or Y@C_{82}; n = 4, 5, 6, 8, or 10).[3,14,16] This interpretation, first proposed in 2003 for C_1-$C_{60}(CF_3)_6$ and C_s- and C_1-$C_{60}(CF_3)_4$,[3] has been challenged by others who propose that the CF_3 groups are arranged on a string or strings of contiguous (i.e., adjacent) sp^3 cage-carbon atoms.[5–7] However, the recently published *pmp*^{3}*mpmp*-, p^7-, and p^7mp-ribbon structures of C_1-$C_{60}(CF_3)_{10}$,[14] C_s-$C_{70}(CF_3)_8$,[26] and C_1-$C_{70}(CF_3)_{10}$,[15] respectively, the similarity of their ^{19}F NMR spectroscopic δ and $^{6,7}J_{F,F}$ values to the corresponding values for all previously reported fullerene$(CF_3)_n$ derivatives,[3,5–7,16] and additional DFT calculations[15] now leave little doubt that ribbon structures are the most common, and in most cases probably the most stable, structures for the high-temperature fullerene$(CF_3)_n$ derivatives reported prior to the present work.

The NMR spectroscopic data and DFT calculations reported here are entirely consistent with 1,4-addition for the abundant isomer of $C_{70}(CF_3)_2$ isolated from the 520 °C residue and with ribbon structures for the abundant $C_{70}(CF_3)_{4,6,8,10}$ isomers isolated from the $\geq$420 °C sublimates. Fluorine-19 δ and $^{6,7}J_{F,F}$ values are listed in Table 4 along with 2D gCOSY correlations for C_1-*pmp*-1-$C_{70}(CF_3)_4$, C_s-p^7-$C_{70}(CF_3)_8$, C_2-p^7-$C_{70}(CF_3)_8$, and C_1-p^7mp-$C_{70}(CF_3)_{10}$ (the addition pattern assigned to each $C_{70}(CF_3)_n$ compound will be discussed in turn below). One-dimensional ^{19}F NMR spectra for five of the six compounds are shown in Figure 6, and 2D gCOSY ^{19}F NMR spectra of C_1-*pmp*-1-$C_{70}(CF_3)_4$ and C_s-p^7-$C_{70}(CF_3)_8$ are shown in Figure 7. The 2D gCOSY ^{19}F NMR spectrum of C_1-p^7mp-$C_{70}(CF_3)_{10}$ was previously published.[14]

A general observation is that CF_3 groups at either terminus of a ribbon of edge-sharing $C_6(CF_3)_2$ hexagons are shielded relative to the CF_3 groups on the interior of the ribbon. This is also true for $C_{60}(CF_3)_n$ derivatives.[3,5,6,14,16] Another general observation is that the $^7J_{F,F}$ values listed in Table 4 for terminal CF_3 groups (these are the only $^{6,7}J_{F,F}$ values for these compounds that are known with a precision of $\pm$0.2 Hz) have a relatively narrow range of values, from 10.3(2) to 16.2(2) Hz. The $J_{F,F}$ coupling between CF_3 groups in *meta*- and *para*-$C_6(CF_3)_2$ hexagons on fullerene$(CF_3)_n$ derivatives is mediated predominantly, if not almost exclusively, by through-space Fermi-contact coupling, as discussed elsewhere.[14,29] This coupling is believed to be due to the overlap of lone-pair electrons between pairs of proximate fluorine atoms.[30] In the case of fullerene$(CF_3)_n$ compounds, a single fluorine atom from a rapidly rotating CF_3 group is positioned over the $C_6(CF_3)_2$ hexagon, putting it in close contact (ca. 2.5–2.8 Å) with a single fluorine atom from a nearest-neighbor rapidly rotating CF_3 group, as shown in Figure 8 for the two terminal *para*-$C_6(CF_3)_2$ hexagons in C_1-p^7mp-$C_{70}(CF_3)_{10}$.[15] Due to the rapid rotation of the CF_3 groups, the observed, time-averaged $^7J_{F,F}$ values listed in Table 4 are nine times smaller than the expected coupling constants for a pair of fluorine atoms frozen into the trapezoid-like arrangements of C–F bonds shown in Figure 8. Therefore, instantaneous $^7J_{F,F}$ values for the two proximate

Table 3. AM1- and DFT-determined relative ΔH_f° values (in kJ mol^{-1}) for selected $C_{70}X_{2,4,6,8,10}$ derivatives.[a]

X	C_1-7,24-$C_{70}X_2$ 6 dbip	C_s-8,23-$C_{70}X_2$ 6 dbip	C_2-1,4-$C_{70}X_2$ 4 dbip	C_s-1,11-$C_{70}X_2$ 3 dbip
H (AM1)	6.0 (6.0)	21.4 (21.4)	0.0 (0.0)	92.4 (92.3)
H (DFT)	7.9	12.5	0.0	29.7
CF_3 (DFT)	**0.0**	**5.1**	**9.1**	**24.0**
X	C_s-p^3-1-$C_{70}X_4$ 7 dbip	C_1-*pmp*-1-$C_{70}X_4$ 7 dbip	C_s-p^3-2-$C_{70}X_4$ 3 dbip	7,8,22,25-$C_{70}X_4$ 5 dbip
H (AM1)	41.0 (41.0)	29.0	0.0 (0.0)	25.1 (25.1)
H (DFT)	34.0	22.6	0.0	−43.8
F (DFT)			0.0	−23.6
Cl (DFT)			0.0	43.2
Br (DFT)	19.7	15.3	0.0	72.4
CF_3 (DFT)	**0.0**	**1.0**	**6.9**	**129.4**
X	C_2-p^5-$C_{70}X_6$ 2 dbip	C_s-p^2,p^2-$C_{70}X_6$ 2 dbip	C_1-p^3*mp*-$C_{70}X_6$ 3 dbip	C_s-p^5-$C_{70}X_6$ 4 dbip
H (AM1)	0.0 (0.0)	48.1	17.6	76.0 (76.6)
H (DFT)	0.0	32.4	20.6	56.6
Ph (AM1)	0.0	44.4 [0]	11.4	76.7 [3×10^1][b]
Ph (DFT)	0.0	29.8	16.6	56.8
F (DFT)	0.0	28.7		
Cl (DFT)	0.0	28.0		
Br (DFT)	0.0	27.6	17.4	52.4
CF_3 (DFT)	**0.0**	**4.0**	**12.6**	**42.1**
X	C_s-p^7-$C_{70}X_8$ 1 dbip	C_2-p^7-$C_{70}X_8$ 2 dbip	C_1-p^5*mp*-$C_{70}X_8$ 3 dbip	C_2-*pmp*,*pmp*-$C_{70}X_8$ 7 dbip
H (AM1)	0.0	34.7		91.0
H (DFT)	0.0	21.6		90.1
Br (DFT)	0.0	19.6		68.9
CF_3 (DFT)	**0.0**	6.0	22.9	24.6

X	C_1-p^7mp-$C_{70}X_{10}$ 2 dbip	C_s-p^9*o*-loop-$C_{70}X_{10}$ 0 dbip	C_2-p^9-$C_{70}X_{10}$ 0 dbip
Br (DFT)	14.7	0.0	14.2
CF_3 (DFT)	**0.0**	**12.4**	**12.3**

[a] All relative ΔH_f° values from this work unless otherwise noted. Abbreviations: dbip = double bonds in pentagons; *p* = *para*-C_6X_2 hexagon; *m* = *meta*-C_6X_2 hexagon; C_s-p^3-1 = 8,23,27,44; C_1-*pmp*-1 = 7,24,44,47; C_s-p^3-2 = 1,4,11,31; C_2-p^5 = 1,4,11,19,31,51; C_s-p^2p^2 = 1,4,11,58,61,64; C_1-p^3mp = 1,4,10,23,25,44; C_s-p^5 = 1,4,11,19,31,51; C_s-p^7 = 1,4,11,19,31,41,51,64; C_2-p^7 = 1,4,11,19,31,41,51,60; C_1-p^5mp = 1,4,10,19,25,41,60,69; C_s-*pmp*,*pmp* = 7,17,24,36,44,47,53,56; C_1-p^7mp = 1,4,10,19,25,41,49,60,66,69; C_s-p^9o-loop = 1,4,11,19,29,41,49,60,66,69; C_2-p^9 = 1,4,11,19,31,41,49,60,66,69. Values in parentheses are from ref. [20]; values in square brackets are from ref. [27]. [b] The difference $\Delta H_f^\circ(C_s$-p^5-$C_{70}Ph_6)-\Delta H_f^\circ(C_s$-$p^2$,$p^2$-$C_{70}Ph_6)$ at the MNDO level was reported to be 13.2 kJ mol^{-1} in ref. [28].

fluorine atoms on nearest-neighbor CF_3 groups in the C_{70}-$(CF_3)_{2,4,6,8,10}$ compounds examined in this study range from 93(2) to 146(2) Hz, and instantaneous $^7J_{F,F}$ values for fluorine atoms significantly more than 3.0 Å apart on different CF_3 groups are approximately 0 Hz.

Fullerene $C_{70}(CF_3)_{10}$: The ^{19}F NMR spectrum of the isomer of $C_{70}(CF_3)_{10}$ isolated in this work by fractional sublimation at 420–480 °C of the 340 °C C_{70}/AgTFA reaction mixture is identical to the spectrum of C_1-p^7mp-$C_{70}(CF_3)_{10}$ prepared at 470 °C by the reaction of C_{70} with CF_3I in a hot tube.[14] Its addition pattern was determined by X-ray crystallography[15] and is shown in Figure 9. This high-temperature addition pattern is unprecedented for $C_{70}X_{10}$ derivatives with X = H,[31] Cl,[23] Br,[32] Me,[33] Ph,[25] and *t*BuOO,[34] all of which were prepared at approximately 25 °C. For X = H, Cl, Br, Me, and Ph, the observed $C_{70}X_{10}$ isomers all have the C_s-p^9o-loop structure shown in Figure 5; for X = *t*BuOO, the isolated isomer has the C_2-p^9 structure shown in Figure 5.

The DFT-predicted relative ΔH_f° values for C_1-p^7mp-, C_s-p^9o-loop-, and C_2-p^9-$C_{70}(CF_3)_{10}$ are 0.0, 12.4, and 12.3 kJ mol^{-1}, respectively (the corresponding values at the AM1 level are 0.0, 36.2, and 22.1 kJ mol^{-1}, respectively[15]). In other words, the stable structure of the high-temperature, high-yield isomer of $C_{70}(CF_3)_{10}$ is not the common low-temperature p^9o-loop-$C_{70}X_{10}$ structure. At the AM1 level, the C_s-p^9o-loop isomer was predicted to be the most stable of the three isomers for X = H, F, Cl, and *t*BuOO, but the p^7mp isomer was predicted to be the most stable of the three isomers not only for X = CF_3 but also for X = Br and Ph.[15] At the DFT level, however, we now find that C_s-p^9o-loop-$C_{70}Br_{10}$ is predicted to be 14.7 kJ mol^{-1} more stable than C_1-p^7mp-$C_{70}Br_{10}$. Nevertheless, it is possible that some C_s-p^9o-loop-$C_{70}X_{10}$ isomers prepared at temperatures significantly below 400 °C may be kinetically stable but not thermodynamically stable with respect to isomerization. This may prove difficult to verify experimentally, at least with thermal-treatment experiments, because, with the exception of a few fluorofullerenes,[35] fullerene$(CF_3)_n$ compounds are the only exohedral fullerene derivatives that do not decompose at temperatures between 400 and 500 °C.

Note that the C_1-p^7mp-$C_{70}(CF_3)_{10}$ isomer is more stable than the C_s-p^9o-loop- and C_2-p^9- alternatives even though it has two destabilizing double bonds in pentagons and the C_s-p^9o-loop- and C_2-p^9- isomers have none. Therefore, the greater stability of the C_1 isomer is probably due to the fact that two bulky CF_3 groups can be farther apart on a *para*-$C_6(CF_3)_2$ hexagon in the more highly curved polar region of the C_{70} cage than on a relatively flat equatorial hexagon, as discussed elsewhere.[15] (The greater steric demands of a CF_3 group relative to a Br atom is well documented.[14]) Nevertheless, the C_1-p^7mp-$C_{70}(CF_3)_{10}$ isomer also has a *meta*-$C_6(CF_3)_2$ hexagon, which, by the same steric argument, would be thought to be destabilizing. However, this may be mitigated by the fact that both CF_3 groups in the *meta*-$C_6(CF_3)_2$

Table 4. Fluorine-19 NMR spectroscopic data.[a]

	C_1-7,24-$C_{70}(CF_3)_2$									
multiplet	a	b			a	b	c	d		
$-\delta$ [ppm]	67.8[b]	68.5[b]			65.6	66.2	66.8[b]	69.1[b]		
COSY[c]					b,d	a,c	b	a		
obsd $J_{F,F}$ [Hz]	12.2	12.2			(10.3), –[d]	(15.9), –[d]	13.3	11.4		
C_{70} locant					C24	C44	C47	C7		
	C_2-p^5-$C_{70}(CF_3)_6$									
multiplet	a	b	c							
$-\delta$ [ppm]	61.9	62.6	66.6[b]							
$J_{F,F}$ [Hz]	–[d]	(16.2), –[d]	16.2							
C_{70} locant	C1/C4	C11/C19	C31/C41							
	C_s-p^7-$C_{70}(CF_3)_8$				C_2-p^7-$C_{70}(CF_3)_8$					
multiplet	a	b	c	d	a	b	c	d		
$-\delta$ [ppm]	61.9	62.0	62.3	66.4[b]	61.8	62.4	63.6	69.2[b]		
COSY[c]	b	a,c	b,d	c	b	a,c	b,d	c		
$J_{F,F}$ [Hz]	–[d]	–[d]	(16.1), –[d]	16.1	–[d]	–[d]	(11.3), –[d]	11.3		
C_{70} locant	C1/C11	C4/C31	C19/C51	C41/C64	C1/C4	C11/C19	C31/C41	C51/C60		
	C_1-p^7mp-$C_{70}(CF_3)_{10}$									
multiplet	a	b	c	d	e	f	g	h	i	j
$-\delta$ [ppm]	59.2	61.5	62.1	62.2	62.4	62.8	63.4	64.3	67.6[b]	70.7[b]
COSY[c]	c,g	e,f	a,h	e,i	b,d	b,g	a,f	c,j	d	h
$J_{F,F}$ [Hz]	–[d]	–[d]	–[d]	(15.9), –[d]	–[d]	–[d]	–[d]	(10.3), –[d]	15.9	10.3
C_{70} locant	C4	C60	C1	C66	C69	C41	C19	C10	C49	C25

[a] All data from this work; solutions in [D$_6$]benzene at 25 °C; C_6F_6 internal std ($\delta = -164.9$ ppm); coupling constants are known to ± 0.2 Hz for terminal CF_3 quartets; coupling constants for apparent septets (quartets of quartets) or unresolved multiplets could not be determined precisely; $J_{F,F}$ values in parentheses were not measured directly but were taken from the COSY-correlated quartet. IUPAC lowest-locant abbreviations: C_1-*pmp*-1 = 7,24,44,47; C_2-p^5 = 1,4,11,19,31,41; C_s-p^7 = 1,4,11,19,31,41,51,64; C_2-p^7 = 1,4,11,19,31,41,51,60; C_1-p^7mp = 1,4,10,19,25,41,49,60,66,69. [b] Terminal CF_3 group. [c] Resonance(s) of gCOSY correlations. [d] The dash denotes that the $J_{F,F}$ value was not determined precisely due to the complexity of the multiplet.

hexagon in the X-ray structure of C_1-p^7mp-$C_{70}(CF_3)_{10}$ are staggered[15] (as are the CF_3 groups in a *meta*-$C_6(CF_3)_2$ hexagon in the X-ray structure of C_1-$C_{60}(CF_3)_{10}$[14]), whereas the CF_3 groups on the equatorial p^7 part of the ribbon in C_1-p^7mp-$C_{70}(CF_3)_{10}$ alternate between the staggered and the (presumably destabilizing) eclipsed conformations. Furthermore, the F$_3$C···CF$_3$ distance for the *meta*-$C_6(CF_3)_2$ hexagon in C_1-p^7mp-$C_{70}(CF_3)_{10}$, at 3.806(3) Å, is only marginally shorter than the approximately 3.94 Å F$_3$C···CF$_3$ distances for several of the equatorial belt *para*-$C_6(CF_3)_2$ hexagons in that structure.[15]

Clare and Kepert realized that the greater complexity (i.e., the lower symmetry) of the $C_{70}X_n$ cage relative to the $C_{60}X_n$ cage leads to "a greater uncertainty [that] all of the most stable isomers have been located" (i.e., have been calculated).[20] Isomers of $C_{70}X_n$ with $n \leq 10$ having ribbons of edge-sharing *meta*- and *para*-C_6X_2 hexagons containing –*para*–*meta*–*para*– sequences were not considered prior to the discovery of the structure of p^7mp-$C_{70}(CF_3)_{10}$, although Clare and Kepert did consider a p^9mp ribbon as a possible addition pattern for $C_{70}H_{12}$ (and found that it was ca. 40 kJ mol^{-1} less stable than the most stable AM1 isomer).[20] We expect that the high-temperature stability of fullerene-$(CF_3)_n$ derivatives, which is virtually unparalleled in exohedral fullerene chemistry, will help to guide future theoretical studies toward other relatively stable, but as yet unknown, addition patterns.

The observation that different high-temperature reactions involving the likely intermediacy of $^{\bullet}CF_3$ radicals (shown in Scheme 1) yield the same abundant isomer of $C_{70}(CF_3)_{10}$, which is predicted to be thermodynamically more stable than $C_{70}(CF_3)_{10}$ isomers with other, more commonly observed addition patterns, suggests that C_1-p^7mp-$C_{70}(CF_3)_{10}$ may be the stable isomer for the fullerene composition C_{70}-$(CF_3)_{10}$, not just the most stable of the three isomers investigated by quantum-chemical calculations. Significantly, the addition patterns assigned to four of the five other abundant, high-temperature isomers isolated and studied in this work are fragments of the C_1-p^7mp-$C_{70}(CF_3)_{10}$ addition pattern, and all five of these assigned addition patterns are predicted by the DFT calculations to be either 1) the most stable structure considered for each $C_{70}(CF_3)_n$ composition or 2) within 1.0 kJ mol^{-1} of the most stable structure.

The two $^7J_{F,F}$ coupling constants for the terminal CF_3 groups in C_1-p^7mp-$C_{70}(CF_3)_{10}$, 10.3(2) and 15.9(2) Hz, can be understood as arising from different F···F distances in the polar *para*-$C_6(CF_3)_2$ hexagon containing C25 and the equatorial *para*-$C_6(CF_3)_2$ hexagon containing C49, 2.744(2) and 2.569(2) Å, respectively (see Figure 8). The larger $^7J_{F,F}$ value is assigned to the equatorial terminal *para*-$C_6(CF_3)_2$ hexagon because of the shorter F···F distance and because of the significantly larger F–C···C–F torsion angle. Larger torsion angles have recently been shown to be correlated with

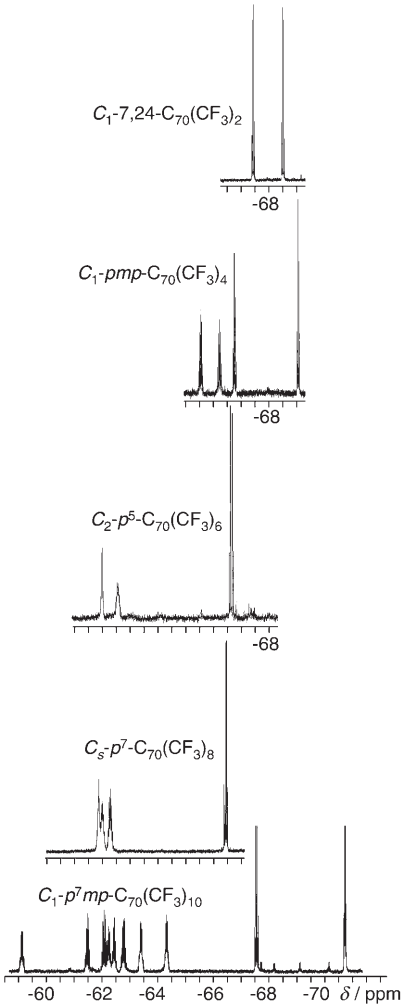

Figure 6. Fluorine-19 NMR spectra of $C_{70}(CF_3)_n$ (n = 2, 4, 6, 8, 10; 376.5 MHz, 25 °C, C_6D_6, $\delta(C_6F_6$ internal std) = −164.9 ppm). The spectrum of p^7*mp*-$C_{70}(CF_3)_{10}$ is reproduced from ref. [14] but the spectrum of a sample of $C_{70}(CF_3)_{10}$ isolated in this work was identical except for more intense peaks due to one or more impurities.

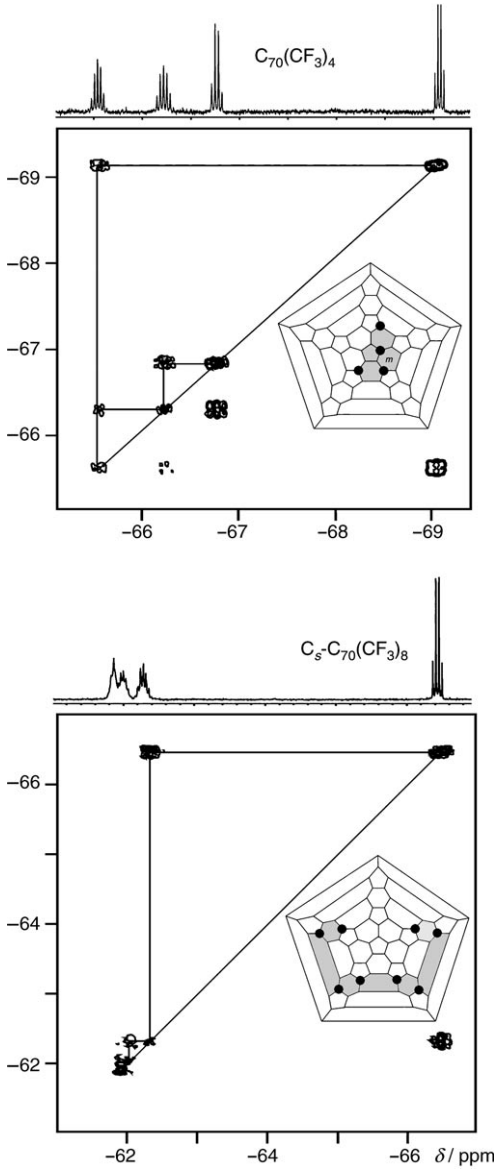

Figure 7. 2D gCOSY ^{19}F NMR spectra of C_1-*pmp*-$C_{70}(CF_3)_4$ and C_s-p^7-$C_{70}(CF_3)_8$ (376.5 MHz, 25 °C, C_6D_6, $\delta(C_6F_6$ internal std) = −164.9 ppm). The proposed structure for each compound is shown in the Schlegel diagram.

larger through-space Fermi-contact $J_{F,F}$ values for a given F···F distance in related $C_{60}F_n(CF_3)$ compounds.[29]

Fullerene $C_{70}(CF_3)_8$: Two isomers were isolated and studied by 1D and 2D ^{19}F NMR spectroscopy. Both exhibit NMR spectra with four CF_3 multiplets, only one of which is a simple quartet. This is consistent with four pairs of symmetry-related CF_3 groups on a single ribbon of seven $C_6(CF_3)_2$ hexagons having either C_s or C_2 symmetry. (Isomers with C_i and C_{2h} symmetry are not possible for $C_{70}X_n$ derivatives, and C_{2v} isomers would exhibit only two ^{19}F multiplets, not four.) An expanded view of the 1D ^{19}F NMR spectrum of the more abundant of the two isomers, which has recently been shown to be the equatorial-belt ribbon isomer C_s-p^7-$C_{70}(CF_3)_8$ by means of single-crystal X-ray crystallography,[26] is shown in Figure 10. The end-of-ribbon CF_3 groups labeled "d" give rise to the quartet at δ = −66.4 ppm with a time-averaged coupling constant of 16.1 Hz. Multiplets "b" and "c" are quartets of quartets (with similar $^7J_{F,F}$ values) due to coupling to two nearest-neighbor CF_3 groups. As expected, the multiplet due to the CF_3 groups labeled "a" is deceptively simple due to the time-averaged chemical-shift equivalence of these CF_3 groups. Interestingly, the DFT-optimized structures of both C_s-p^7-$C_{70}(CF_3)_8$ and C_2-p^7-$C_{70}(CF_3)_8$ have only idealized C_s and C_2 symmetry, respectively. Both structures are asymmetric due to variations in CF_3 conformations. For example, in both DFT-optimized structures (and in the X-ray structure of the C_s isomer[26]) one of the two middle CF_3 groups (labeled a in Figure 10) is almost perfectly staggered and the other is nearly eclipsed. This is not true for DFT-optimized structures of C_s-p^7-$C_{70}X_8$ and C_2-p^7-$C_{70}X_8$ with monatomic substituents such as H and Br, which have

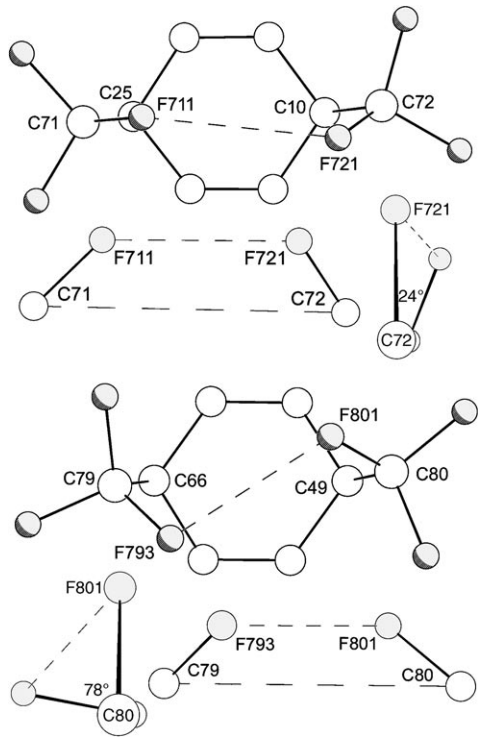

Figure 8. The trapezoid-like arrangement of pairs of C–F bonds for the terminal *para*-$C_6(CF_3)_2$ hexagons in the X-ray structure of C_1-p^7mp-$C_{70}(CF_3)_{10}$ reported in ref. [15]. The F711···F721 and C71···C72 distances are 2.744(2) and 4.412(3) Å, respectively, and the time-averaged $^7J_{F,F}$ value for these CF_3 groups is 10.3(2) Hz. The F793···F801 and C79···C80 distances are 2.570(2) and 3.935(3) Å, respectively, and the time-averaged $^7J_{F,F}$ value for these two CF_3 groups is 15.9(2) Hz. The angles shown are F-C···C-F torsion angles.

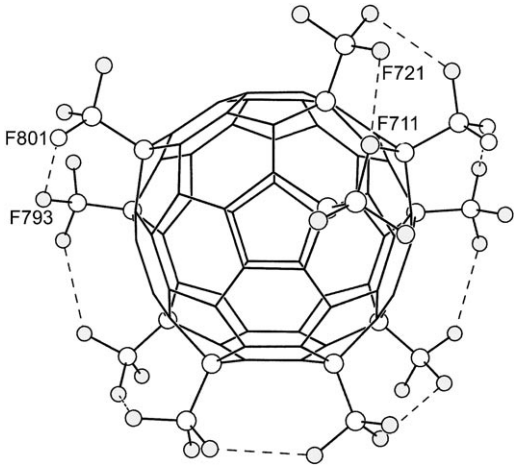

Figure 9. Drawing of C_1-p^7mp-$C_{70}(CF_3)_{10}$ determined by X-ray crystallography and reported in ref. [15], looking down the original C_5 axis of the empty C_{70} cage. The smaller spheres are fluorine atoms. The F793···F801 and F711···F721 distances are 2.570(2) and 2.744(2) Å, respectively. The other F···F distances shown range from 2.513(2) to 2.744(2) Å.

rigorous C_s or C_2 symmetry. It will be interesting to see, in future work, if the presumed rapid equilibration of the two

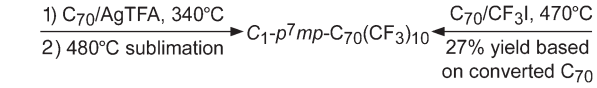

Scheme 1. Equation showing that different high-temperature reactions yield the same abundant isomer of $C_{70}(CF_3)_{10}$.

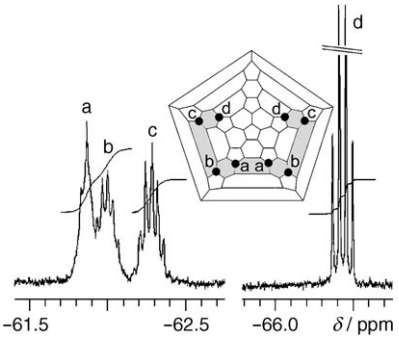

Figure 10. Expansions of the ^{19}F NMR spectrum of C_s-p^7-$C_{70}(CF_3)_8$ (376.5 MHz, 25 °C, C_6D_6, $\delta(C_6F_6$ internal std) = −164.9 ppm), showing the quartet, two quartets of quartets, and an unresolved multiplet. The observed $^7J_{F,F}$ value for quartet d is 16.1(2) Hz. The spectrum of C_2-p^7-$C_{70}(CF_3)_8$ (not shown) is nearly identical to this spectrum except that the $^7J_{F,F}$ value for quartet d is 11.3(2) Hz.

enantiomeric conformers of C_s-p^7-$C_{70}(CF_3)_8$ and C_2-p^7-$C_{70}(CF_3)_8$ can be slowed enough at a sufficiently low temperature so that eight multiplets are observed in slow-exchange-limit ^{19}F NMR spectra instead of only four.

The ^{19}F NMR spectrum of the less abundant isomer C_2-p^7-$C_{70}(CF_3)_8$ (not shown) is virtually identical except that the time-averaged $^7J_{F,F}$ value for quartet d is only 11.3(2) Hz. This is a more significant difference relative to the time-averaged 16.1(2) Hz $^7J_{F,F}$ value for the C_s isomer than it may appear because the instantaneous $^7J_{F,F}$ values are 102(2) and 145(2) Hz and therefore differ by 43 Hz. The difference is probably because the DFT-optimized F···F distances involving the CF_3 groups on the end-of-ribbon *para*-$C_6(CF_3)_2$ hexagons in the C_2 isomer (2.69 and 2.81 Å) are longer than the corresponding distances in the C_s isomer (2.57 and 2.69 Å). In addition, the FC···CF torsion angles for the end-of-ribbon hexagons in the C_2 isomer (28 and 51°) are smaller than the corresponding torsion angles in the C_s isomer (69 and 76°).

The results in Table 3 show that the DFT-determined ΔH_f° values for C_s- and C_2-p^7-$C_{70}(CF_3)_8$ only differ by 6.0 kJ mol^{-1}. In contrast, the $\Delta\Delta H_f^\circ$ values for C_s- and C_2-p^7-$C_{70}H_8$ and for C_s- and C_2-p^7-$C_{70}Br_8$ are 21.6 and 19.6 kJ mol^{-1}, respectively. We believe the smaller difference for the trifluoromethyl derivatives is because of greater steric hindrance in the C_s isomer, which should be a more important factor for a large substituent like CF_3 relative to Br or H.[14] The DFT-optimized structure shows that C_s-p^7-$C_{70}(CF_3)_8$ has four shorter F_3C···CF_3 distances (3.96–4.06 Å) and three longer F_3C···CF_3 distances (4.28–4.32 Å). In contrast, the C_2 isomer has three shorter F_3C···CF_3 distances (3.95–3.98 Å) and four longer F_3C···CF_3 distances (4.28–4.43 Å). The different F_3C···CF_3 distances, in turn, are due

to different tilt angles of the $F_3C{-}C_{cage}$ vectors with respect to the *para*-$C_6(CF_3)_2$ hexagon in question, and are observed in the X-ray structures of C_s-p^7-$C_{70}(CF_3)_8$,[26] C_1-p^7mp-$C_{70}(CF_3)_{10}$,[14] and C_s-p^7-$C_{70}Me_8$.[36]

Other $C_{70}X_8$ derivatives that have been shown (spectroscopically) to have the C_s-p^7 addition pattern include $C_{70}H_8$,[37] $C_{70}Ph_8$,[25] and $C_{70}(t\text{BuOO})_8$.[38] If our assignment of the C_2-p^7 equatorial-ribbon structure to the less abundant isomer of $C_{70}(CF_3)_8$ is correct, this would be the first observation of this addition pattern for any $C_{70}X_8$ derivative. There may be a kinetic preference, at ambient temperature, for the quenching of a putative $C_{70}X_7$ radical with another $X^{\bullet}$ radical to form the C_s-p^7-$C_{70}X_8$ structure instead of the C_2-p^7-$C_{70}X_8$ structure. The only example in the literature of apparent sequential radical addition to C_{70} to yield an isolable $C_{70}X_8$ derivative is $C_{70}+n(t\text{BuOO}^{\bullet})\rightarrow C_{70}(t\text{BuOO})_n$, recently reported by Gan and co-workers, and the only isomer of $C_{70}(t\text{BuOO})_8$ that was formed was C_s-p^7-$C_{70}(t\text{BuOO})_8$.[38] Perhaps it is the combination of the large size of the CF_3 group and the application of temperatures $\geq 400\,^{\circ}C$ that has allowed an isomer of $C_{70}(CF_3)_8$ with the unprecedented C_2-p^7 addition pattern to be formed. In contrast to the case of $C_{70}(CF_3)_{10}$, the most stable isomer of $C_{70}(CF_3)_8$ does have the fewest double bonds in pentagons.

Fullerene $C_{70}(CF_3)_6$: The ^{19}F NMR spectrum of the abundant isomer of $C_{70}(CF_3)_6$ is topologically similar to the spectra of the two $C_{70}(CF_3)_8$ isomers except that only one apparent septet (quartet of quartets) was observed instead of two. This indicates that the isolated isomer contains a single ribbon with C_s or C_2 symmetry, and the lowest energy isomer in Figure 5 that fits the NMR spectroscopic data is C_2-p^5-$C_{70}(CF_3)_6$. This isomer, which has the fewest double bonds in pentagons of all those considered, is consistent with the 16.2(2) Hz time-averaged $^7J_{F,F}$ value for the end-of-ribbon *para*-$C_6(CF_3)_2$ hexagons, because the relevant DFT-optimized F···F and $F_3C{\cdots}CF_3$ distances and F-C···C-F torsion angles for this isomer (F···F, 2.57 and 2.68 Å; $F_3C{\cdots}CF_3$, 4.00 and 4.07 Å; F-C···C-F, 70 and 77°) are virtually the same as the corresponding parameters for C_s-p^7-$C_{70}(CF_3)_8$ ($^7J_{F,F}$ = 16.1(2) Hz) and for the equatorial end-of-ribbon *para*-$C_6(CF_3)_2$ hexagon in C_1-p^7mp-$C_{70}(CF_3)_{10}$ ($^7J_{F,F}$ = 15.9(2) Hz). The alternative C_s-p^5-$C_{70}(CF_3)_6$ and C_2-*pmpmp*-$C_{70}(CF_3)_6$ isomers are ruled out not only because they are higher in energy but because their structures would be commensurate with $^7J_{F,F}$ values in the 10–12 Hz range. As was the case for the DFT-optimized C_s-p^7 and C_2-p^7 isomers of $C_{70}(CF_3)_8$, the DFT-optimized structure of C_2-p^5-$C_{70}(CF_3)_6$ possesses only idealized C_2 symmetry. Its true instantaneous structure is asymmetric, and the NMR spectrum reflects the fact that the enantiomeric conformers are rapidly equilibrating on the NMR spectroscopic timescale.

A small amount of a C_1-symmetry isomer of $C_{70}(CF_3)_6$ prepared at 300 °C has been reported.[7] Its ^{19}F NMR spectrum exhibited two end-of-ribbon quartets with $J_{F,F}$ values of 17.2 and 12.0 Hz (errors for the $J_{F,F}$ values were not given).[7] No structural assignment was made at that time. However, based on the results reported in this paper concerning $C_{70}(CF_3)_n$ derivatives in general, the reported $^7J_{F,F}$ values are precisely what one would now expect for the C_1-p^3mp-$C_{70}(CF_3)_6$ isomer shown in Figure 5 (i.e., 16 ± 1 Hz and 11 ± 1 Hz), so this relatively low-energy isomer may correspond to the isomer prepared at 300 °C. It will be interesting to see if the presumed C_1-p^3mp-$C_{70}(CF_3)_6$ isomer undergoes isomerization to C_2-p^5-$C_{70}(CF_3)_6$ above 400 °C.

The compound C_2-p^5-$C_{70}(t\text{BuOO})_6$ is one of only two other $C_{70}X_6$ derivatives to be isolated and characterized by reliable physicochemical techniques,[38] and is the only compound other than C_2-p^5-$C_{70}(CF_3)_6$ that has been recognized to exhibit the C_2-p^5-$C_{70}X_6$ structure. There may be an unrecognized example, however. An isomer of $C_{70}Ph_6$ was the subject of several papers in 2000 and 2001.[27,28,39] The reported NMR spectroscopic data demonstrated that the phenyl groups were arranged to give three symmetry-related pairs. For reasons that are not clear, the authors considered only the C_s-p^5-$C_{70}X_6$ and C_s-p^2,p^2-$C_{70}X_6$ addition patterns as possibilities for their compound. They either ignored or were not aware of the fact that the C_2-p^5-$C_{70}X_6$ addition pattern was not only predicted by Clare and Kepert in 1999 to be more stable than the two C_s isomers for X = H, it also fit all of the reported data better than either of the two C_s structures. For example, in one paper the mismatch between the number of sp^2 ^{13}C resonances for $C_{70}Ph_6$ and the number expected for the "most likely" C_s-p^5 structure was explained away as "probably due to signal coincidence" despite the fact that the C_2-p^5 structure would naturally give rise to fewer signals.[28] Furthermore, in another paper the small S_0–S_1 energy gap predicted[27] for C_s-p^5-$C_{70}Ph_6$ required that its fluorescence at 728 nm was due to a highly unusual radiative relaxation from an S_2 state instead of from the S_1 state.[27] Our DFT HOMO–LUMO gaps for C_s-p^5- and C_2-p^5-$C_{70}Ph_6$ are 0.49 and 1.41 eV, respectively, so once again the reported data are better explained by assuming that the isomer of $C_{70}Ph_6$ that has been isolated and studied in the past[27,28,39] is in fact the C_2-p^5 isomer.

Fullerene $C_{70}(CF_3)_4$: The ^{19}F NMR spectrum of the abundant isomer of $C_{70}(CF_3)_4$ is significantly different from the spectra of C_s- and C_2-p^7-$C_{70}(CF_3)_8$ and C_2-p^5-$C_{70}(CF_3)_6$ in that there are two simple quartets, with $^7J_{F,F}$ values of 11.4 and 13.3 Hz, and two quartets of quartets (apparent septets). Together with the correlations observed in the 2D gCOSY spectrum, which require an asymmetric ribbon of three *meta*- and/or *para*-$C_6(CF_3)_2$ edge-sharing hexagons, the only possible structures are various C_1-*pmp*- and C_1-p^3-$C_{70}(CF_3)_4$ isomers. However, all possible C_1-p^3 isomers have a CF_3 group attached to a triple-hexagon junction, and the DFT calculations predict that even the most stable of these is too high in energy to be a viable candidate for the structure of the isolated isomer.

The two lowest-energy C_1-*pmp* isomers, C_1-*pmp*-1-$C_{70}(CF_3)_4$ and C_1-*pmp*-2-$C_{70}(CF_3)_4$, are shown in Figure 5. Both involve the addition of four CF_3 groups to one of the polar regions of C_{70}. Although the equatorial-belt C_s-p^3 isomers of

$C_{70}H_4$ and $C_{70}Br_4$ are predicted to be more stable than the corresponding C_1-*pmp*-1 isomers (see Table 3), the greater bulk of CF_3 groups[14] causes a reversal of this trend (as discussed above, the polar region of C_{70} is more highly curved than the equatorial region and therefore allows CF_3 groups arranged on polar hexagons to be slightly farther apart than on equatorial hexagons).

The C_1-*pmp*-2-$C_{70}(CF_3)_4$ isomer is not only predicted to be 20.4 kJ mol^{-1} higher in energy than the C_1-*pmp*-1-$C_{70}(CF_3)_4$ isomer, its set of DFT-optimized end-of-ribbon $F_3C\cdots CF_3$ distances and F-C···C-F torsion angles would be expected to give rise to quartet $^7J_{F,F}$ values similar to those observed for C_1-p^7*mp*-$C_{70}(CF_3)_{10}$, namely, 10.3(2) and 15.9(2) Hz. Sets of end-of-ribbon $F_3C\cdots CF_3$ distances and F-C···C-F torsion angles are {4.48 Å, 16°} and {4.03 Å, 74°} for C_1-*pmp*-2-$C_{70}(CF_3)_4$ and {4.412(3) Å, 24°} and {3.935(3) Å, 78°} for C_1-p^7*mp*-$C_{70}(CF_3)_{10}$ (X-ray structure[15]).

On the other hand, the DFT-optimized structural parameters for C_1-*pmp*-1-$C_{70}(CF_3)_4$ and the observed coupling constants match very well with the DFT-optimized structural parameters and observed coupling constants for C_1-*pmp*-$C_{60}(CF_3)_4$.[3,4] The ^{19}F NMR spectra for both compounds, including the $^7J_{F,F}$ values for the simple quartets, are compared in Figure 11. Their overall structural similarity can be seen in the Schlegel diagrams also shown in Figure 11. Sets of end-of-ribbon $F_3C\cdots CF_3$ distances and F-C···C-F torsion angles are {4.47 Å, 6.2°} and {4.44 Å, 25°} for C_1-*pmp*-1-$C_{70}(CF_3)_4$ and {4.36 Å, 6.9°} and {4.37 Å, 17°} for C_1-*pmp*-$C_{60}(CF_3)_4$. The preponderance of evidence strongly indicates that the high-temperature abundant isomer of $C_{70}(CF_3)_4$ we have isolated is in fact C_1-*pmp*-1-$C_{70}(CF_3)_4$.

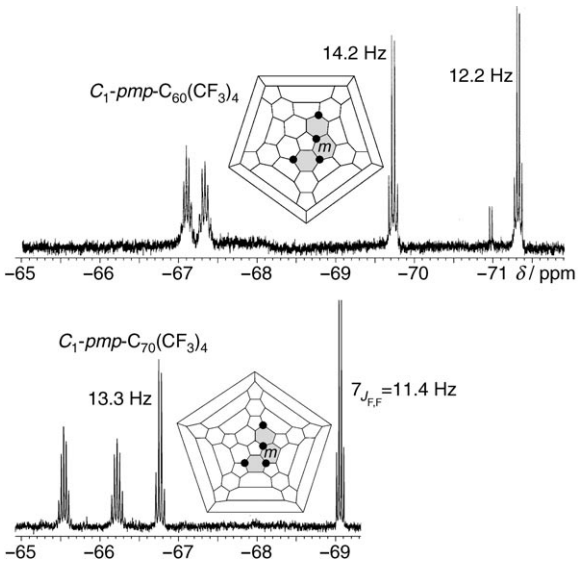

Figure 11. Comparison of the ^{19}F NMR spectra (376.4 MHz, 25 °C, $\delta(C_6F_6$ internal std) = −164.9 ppm) of C_1-*pmp*-$C_{60}(CF_3)_4$ (top; [D_8]toluene) and C_1-*pmp*-1-$C_{70}(CF_3)_4$ (bottom; [D_6]benzene).

One isomer previously isolated from a 300 °C reaction of C_{70} and AgTFA[7] had an ^{19}F NMR spectrum nearly identical to our spectrum of C_1-pmp-1-$C_{70}(CF_3)_4$ but was assigned to a structure with CF_3 groups on four contiguous carbon atoms, namely, 7,8,22,25-$C_{70}(CF_3)_4$.[7] Our calculated DFT relative energy for this isomer is more than 120 kJ mol^{-1} higher than that for the C_1-*pmp*-1 isomer. As we have previously concluded, fullerene$(CF_3)_n$ structures with CF_3 groups on adjacent cage-carbon atoms, if they occur at all, will be rare.[14]

Figure 5 shows two isomers of $C_{70}(CF_3)_4$, chosen at random, that have two isolated *para*-$C_6(CF_3)_2$ hexagons and ΔH_f° values greater than 27 kJ mol^{-1} relative to the most stable isomer, C_s-p^3-1-$C_{70}(CF_3)_2$. Our extensive search of over 1700 $C_{70}(CF_3)_4$ isomers at the AM1 level led to the discovery of seventeen additional *p,p*-$C_{70}(CF_3)_4$ isomers with relative ΔH_f° values of 25.2 kJ mol^{-1} or less. The locant numbers and relative energies of the 21 most stable isomers of $C_{70}(CF_3)_4$ that are based on ribbons of edge-sharing $C_6(CF_3)_2$ hexagons or two isolated *para*-$C_6(CF_3)_2$ hexagons at the DFT level are listed in Table 5.

We also determined the relative ΔH_f° values of other $C_{70}X_4$ derivatives as part of our DFT study, and have discovered that 7,8,22,25-$C_{70}H_4$ and 7,8,22,25-$C_{70}F_4$ are significantly more stable than the corresponding C_2-p^3-2 isomer at the DFT level (see Table 3). This is in contrast to the expectation, based on Clare and Kepert's classic AM1 study, that both C_s-p^3-2-$C_{70}H_4$ and C_s-p^3-2-$C_{70}F_4$ should be the more stable isomers (the AM1 prediction is that C_s-p^3-2-$C_{70}H_4$ is 25.1 kJ mol^{-1} more stable than 7,8,22,25-$C_{70}H_4$).[20] The reason for this reversal is unclear at this time and is under further investigation.

Table 5. Relative DFT ΔH_f° values for the most stable isomers $C_{70}(CF_3)_4$ based on ribbons of edge-sharing $C_6(CF_3)_2$ hexagons or two isolated *para*-$C_6(CF_3)_2$ hexagons.

Isomer designation	IUPAC lowest locants	Relative ΔH_f° [kJ mol^{-1}]
C_s-p^3-1	8,23,27,44	0.0
C_1-*pmp*-1	7,24,44,47	1.0
C_2-*p,p*-1	7,24,32,54	1.3
C_2-*p,p*-2	7,24,36,57	1.3
C_1-*p,p*-1	7,24,34,52	2.2
C_1-*p,p*-2	7,14,24,35	6.3
C_s-p^3-2	1,4,11,31	6.9
C_2-*p,p*-3	7,15,24,34	7.4
C_2-*p,p*-4	7,24,55,67	8.3
C_2-*p,p*-5	7,18,24,35	10.1
C_1-*p,p*-3	1,4,24,43	11.8
C_s-*p,p*-1	7,17,24,36	12.1
C_1-*p,p*-4	7,24,33,53	13.3
C_1-*p,p*-5	1,4,46,62	14.6
C_1-*p,p*-6	1,4,28,46	14.8
C_1-*p,p*-7	1,4,26,48	15.8
C_1-*p,p*-8	1,4,45,63	16.1
C_1-*pmp*-2	1,4,10,25	20.4
C_1-*p,p*-9	1,4,32,54	20.7
C_s-*p,p*-2	1,4,49,66	21.6
C_1-p^2m	1,10,22,25	25.2

Fullerene $C_{70}(CF_3)_2$: The ^{19}F NMR spectrum of the abundant isomer of $C_{70}(CF_3)_2$ consists of two quartets with a $^7J_{F,F}$ value

of 12.2 Hz, indicating C_1 symmetry and the presence of a *para*-$C_6(CF_3)_2$ hexagon in the polar region. The results in Table 3 strongly suggest that this isomer is 7,24-$C_{70}(CF_3)_2$, the second-most stable 1,4-addition pattern for $C_{70}H_2$[20] but the most stable 1,4-addition pattern for $C_{70}(CF_3)_2$ because of the greater steric bulk of CF_3 groups. Note that it contains six double bonds in pentagons (one more than C_{70} itself), three more than the C_s-1,11-isomer, but is 24.0 kJ mol^{-1} more stable than this equatorial belt *para*-$C_6(CF_3)_2$ isomer.

Raman spectra of C_1-*pmp*-1-$C_{70}(CF_3)_4$ and C_s-p^7-$C_{70}(CF_3)_8$: These spectra, shown in Figure 12, are in excellent agreement with the calculated spectra and lend further support to

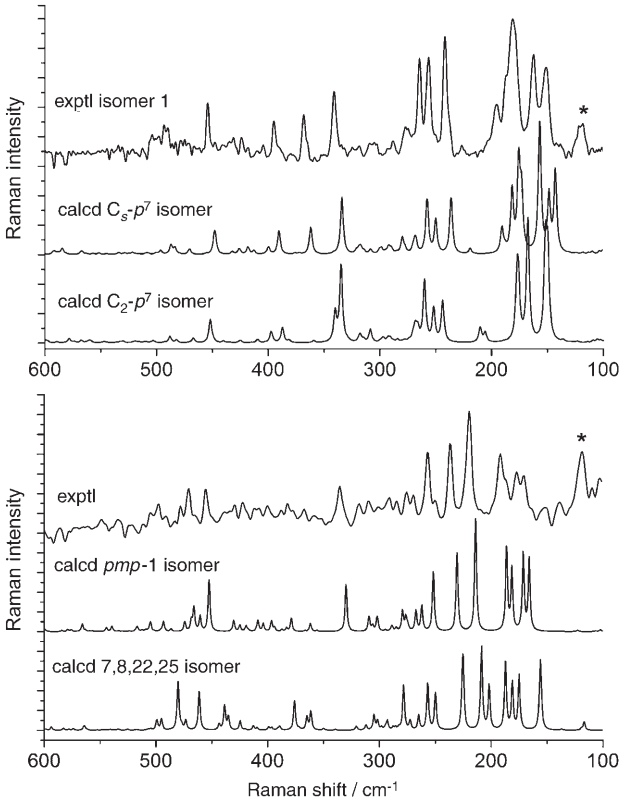

Figure 12. Experimental Raman spectra of the abundant isolated isomers of $C_{70}(CF_3)_4$ (bottom) and $C_{70}(CF_3)_8$ (top) and DFT-calculated Raman spectra of C_1-*pmp*-1- and 7,8,22,25-$C_{70}(CF_3)_4$ and C_s-p^7- and C_2-p^7-$C_{70}(CF_3)_8$.

the structural assignments made on the basis of ^{19}F NMR spectroscopy. Especially noteworthy are the bands in the 140 to 280 cm^{-1} regions, which appear to be very sensitive in position and intensity to the specific addition pattern. In the case of $C_{70}(CF_3)_8$, even the structurally similar C_s-p^7 and C_2-p^7 isomers can be distinguished by their Raman spectra.

Acknowledgements

We thank Professor D. W. Grainger for the use of his HPLC equipment and Term-USA for a gift of C_{70}. This work was supported by the Volkswagen Foundation (I-77/855), RFBR-Grant nos. 03-03-32179 (to A.A.P) and 03-03-32855 and 03-03-32856 (to V.Y.M.), INTAS Young Scientist Fellowships nos. 03-55-1811 (to A.V.S.) and 04-83-3316 (to I.N.I.), and the U.S. National Science Foundation.

[1] I. S. Uzkikh, E. I. Dorozhkin, O. V. Boltalina, A. I. Boltalin, *Dokl. Akad. Nauk* **2001**, *379*, 344–347.
[2] O. V. Boltalina, A. I. Boltalin, I. S. Uzkikh, E. I. Dorozhkin, patent no. 2182897 C1, Khimicheskii Fakul'tet MGU, Russia, **2002**.
[3] A. A. Goryunkov, I. V. Kuvychko, I. N. Ioffe, D. L. Dick, L. N. Sidorov, S. H. Strauss, O. V. Boltalina, *J. Fluorine Chem.* **2003**, *124*, 61–64.
[4] A. A. Goryunkov, I. N. Ioffe, I. V. Kuvychko, T. S. Yankova, V. Y. Markov, A. V. Streletskii, D. L. Dick, L. N. Sidorov, O. V. Boltalina, S. H. Strauss, *Fullerenes, Nanotubes, Carbon Nanostruct.* **2004**, *12*, 181–185.
[5] A. D. Darwish, A. G. Avent, A. K. Abdul-Sada, R. Taylor, *Chem. Commun.* **2003**, 1374–1375.
[6] A. D. Darwish, A. K. Abdul-Sada, A. G. Avent, V. I. Lyakhovetsky, E. A. Shilova, R. Taylor, *Org. Biomol. Chem.* **2003**, *1*, 3102–3110.
[7] A. D. Darwish, A. K. Abdul-Sada, A. G. Avent, N. Martsinovich, J. M. Street, R. Taylor, *J. Fluorine Chem.* **2004**, *125*, 1383–1391.
[8] D. N. Laikov, *Chem. Phys. Lett.* **1997**, *281*, 151–156.
[9] J. P. Perdew, K. Burke, M. Ernzerhof, *Phys. Rev. Lett.* **1996**, *77*, 3865–3868.
[10] A. A. Granovsky, PC GAMESS, http://classic.chem.msu.su/gran/gamess/index.html/.
[11] M. W. Schmidt, K. K. Baldridge, J. A. Boatz, S. T. Elbert, M. S. Gordon, J. H. Jensen, S. Koseki, N. Matsunaga, K. A. Nguyen, S. J. Su, T. L. Windus, M. Dupuis, J. A. Montgomery, *J. Comput. Chem.* **1993**, *14*, 1347–1363.
[12] P. J. Fagan, P. J. Krusic, C. N. McEwen, J. Lazar, D. H. Parker, N. Herron, E. Wasserman, *Science* **1993**, *262*, 404–407.
[13] N. Tagmatarchis, A. Taninaka, H. Shinohara, *Chem. Phys. Lett.* **2002**, *355*, 226–232.
[14] I. E. Kareev, I. V. Kuvychko, S. F. Lebedkin, S. M. Miller, O. P. Anderson, K. Seppelt, S. H. Strauss, O. V. Boltalina, *J. Am. Chem. Soc.* **2005**, *127*, 8362–8375.
[15] I. E. Kareev, I. V. Kuvychko, A. A. Popov, S. F. Lebedkin, S. M. Miller, O. P. Anderson, S. H. Strauss, O. V. Boltalina, *Angew. Chem.* **2005**, *117*, 8198–8201; *Angew. Chem. Int. Ed.* **2005**, *44*, 7984–7987.
[16] I. E. Kareev, S. F. Lebedkin, V. P. Bubnov, E. B. Yagubskii, I. N. Ioffe, P. A. Khavrel, I. V. Kuvychko, S. H. Strauss, O. V. Boltalina, *Angew. Chem.* **2005**, *117*, 1880–1883; *Angew. Chem. Int. Ed.* **2005**, *44*, 1846–1849.
[17] P. W. Fowler, D. B. Redmond, J. P. B. Sandall, *J. Chem. Soc. Faraday Trans.* **1998**, *94*, 2883–2887.
[18] a) A. V. Streletskii, I. N. Ioffe, S. G. Kotsiris, M. P. Barrow, T. Drewello, S. H. Strauss, O. V. Boltalina, *J. Phys. Chem. A* **2005**, *109*, 714–719; b) I. V. Kuvychko, A. V. Streletskii, A. A. Popov, S. G. Kotsiris, T. Drewello, S. H. Strauss, O. V. Boltalina, *Chem. Eur. J.* **2005**, *11*, 5426–5436.
[19] a) M. Baillie, D. Brown, K. Moss, D. Sharp, *J. Chem. Soc. A* **1968**, 3110–3114; b) G. E. Carr, R. D. Chambers, *J. Chem. Soc. Perkin Trans. 1* **1988**, 921–926.
[20] B. W. Clare, D. L. Kepert, *THEOCHEM.* **1999**, *491*, 249–264.
[21] a) H. R. Karfunkel, A. Hirsch, *Angew. Chem.* **1992**, *104*, 1529–1531; *Angew. Chem. Int. Ed. Engl.* **1992**, *31*, 1468–1470; b) C. C. Henderson, C. M. Rohlfing, P. A. Cahill, *Chem. Phys. Lett.* **1993**, *213*, 383–388.
[22] A. G. Avent, A. D. Darwish, D. K. Heimbach, H. W. Kroto, M. F. Meidine, J. P. Parsons, C. Remars, R. Roers, O. Ohashi, R. Taylor, D. R. M. Walton, *J. Chem. Soc. Perkin Trans. 2* **1994**, 15–22.
[23] P. R. Birkett, A. G. Avent, A. D. Darwish, H. W. Kroto, R. Taylor, D. R. M. Walton, *J. Chem. Soc. Chem. Commun.* **1995**, 683–684.
[24] S. J. Austin, P. W. Fowler, J. P. B. Sandall, P. R. Birkett, A. G. Avent, A. D. Darwish, H. W. Kroto, R. Taylor, D. R. M. Walton, *J. Chem. Soc. Perkin Trans. 2* **1995**, 1027–1028.

[25] A. G. Avent, P. R. Birkett, A. D. Darwish, H. W. Kroto, R. Taylor, D. R. M. Walton, *Tetrahedron* **1996**, *52*, 5235–5246.
[26] A. A. Goryunkov, E. I. Dorozhkin, D. V. Ignat'eva, L. N. Sidorov, E. Kemnitz, G. M. Sheldrick, S. I. Troyanov, *Mendeleev Commun.* **2005**, 225–227.
[27] P.-F. Coheur, J. Cornil, D. A. dos Santos, P. R. Birkett, J. Lievin, J. L. Bredas, D. R. M. Walton, R. Taylor, H. W. Kroto, R. Colin, *J. Chem. Phys.* **2000**, *112*, 6371–6381.
[28] A. G. Avent, P. R. Birkett, M. Carano, A. D. Darwish, H. W. Kroto, J. O. Lopez, F. Paoulucci, S. Roffia, R. Taylor, N. Wachter, D. R. M. Walton, F. Zerbetto, *J. Chem. Soc. Perkin Trans. 2* **2001**, 140–145.
[29] I. E. Kareev, G. Santiso Quinones, I. V. Kuvychko, P. A. Khavrel, I. N. Ioffe, I. V. Goldt, S. F. Lebedkin, K. Seppelt, S. H. Strauss, O. V. Boltalina, *J. Am. Chem. Soc.* **2005**, *127*, 11497–11504.
[30] a) Y. G. Gakh, A. A. Gakh, A. M. Gronenborn, *Magn. Reson. Chem.* **2000**, *38*, 551–558; b) F. B. Mallory, C. W. Mallory, K. E. Butler, M. B. Lewis, A. Q. Xia, E. D. Luzik, Jr., L. E. Fredenburgh, M. M. Ramanjulu, Q. N. Van, M. M. Franci, D. A. Freed, C. C. Wray, C. Hann, M. Nerz-Stormes, P. J. Carroll, L. E. Chirlian, *J. Am. Chem. Soc.* **2000**, *122*, 4108–4116; c) J. E. Peralta, V. Barone, R. H. Contreras, D. G. Zaccari, J. P. Snyder, *J. Am. Chem. Soc.* **2001**, *123*, 9162–9163; d) I. Alkorta, J. E. Elguero, *Struct. Chem.* **2004**, *15*, 117–120; e) T. Tuttle, J. Grafenstein, D. Cremer, *Chem. Phys. Lett.* **2004**, *394*, 5–13; f) N. Castillo, C. F. Matta, R. J. Boyd, *J. Chem. Inf. Model* **2005**, *45*, 354–359.
[31] H. P. Spielmann, B. R. Weedon, M. S. Meier, *J. Org. Chem.* **2000**, *65*, 2755–2758.
[32] S. I. Troyanov, A. A. Popov, N. I. Denisenko, O. V. Boltalina, L. N. Sidorov, E. Kemnitz, *Angew. Chem.* **2003**, *115*, 2497–2500; *Angew. Chem. Int. Ed.* **2003**, *42*, 2395–2398.
[33] H. Al-Matar, A. K. A. Sada, A. G. Avent, R. Taylor, X. W. Wei, *J. Chem. Soc. Perkin Trans. 2* **2002**, 1251–1256.
[34] L. B. Gan, S. H. Huang, X. A. Zhang, A. X. Zhang, B. C. Cheng, H. Cheng, X. L. Li, G. Shang, *J. Am. Chem. Soc.* **2002**, *124*, 13384–13385.
[35] O. V. Boltalina, S. H. Strauss in *Dekker Encyclopedia of Nanoscience and Nanotechnology* (Eds.: J. A. Schwarz, C. Contescu, K. Putyera), Marcel Dekker, New York, **2004**, pp. 1175–1190.
[36] A. D. Darwish, P. de Guio, R. Taylor, *Fullerenes, Nanotubes, Carbon Nanostruct.* **2002**, *10*, 261–272.
[37] H. P. Spielmann, G.-W. Wang, M. S. Meier, B. R. Weedon, *J. Org. Chem.* **1998**, *63*, 9865–9871.
[38] Z. Xiao, F. D. Wang, S. H. Huang, L. B. Gan, J. Zhou, G. Yuan, M. J. Lu, J. Q. Pan, *J. Org. Chem.* **2005**, *70*, 2060–2066.
[39] R. V. Bensasson, M. Schwell, M. Fanti, N. K. Wachter, J. O. Lopez, J.-M. Janot, P. R. Birkett, E. J. Land, S. Leach, P. Seta, R. Taylor, F. Zerbetto, *ChemPhysChem* **2001**, *2*, 109–114.

Received: October 31, 2005
Published online: March 21, 2006

